European Journal of Neuroscience, Vol. 10, pp. 718–728, 1998

Gamma frequency oscillation in the hippocampus of the rat: intracellular analysis *in vivo*

Markku Penttonen,[1,2] Anita Kamondi,[1] László Acsády[1,3] and György Buzsáki[1]
[1]Center for Molecular and Behavioural Neuroscience, Rutgers, The State University of New Jersey, 197 University Avenue, Newark, NJ 07102 New Jersey, USA
[2]A. I. Virtanen Institute, University of Kuopio, Kuopio, Finland
[3]Institute of Experimental Medicine, Hungarian Academy of Sciences, Budapest, Hungary

Abstract

Gamma frequency field oscillations reflect synchronized synaptic potentials in neuronal populations within the ~ 10–40 ms range. The generation of gamma activity in the hippocampus was investigated by intracellular recording from principal cells and basket cells in urethane anaesthetized rats. The recorded neurones were verified by intracellular injection of biocytin. Gamma frequency field oscillations were nested within the slower theta waves. The phase and amplitude of intracellular gamma were voltage dependent with an almost complete phase reversal at Cl^- equilibrium potential in pyramidal cells. Basket cells fired at gamma frequency and were phase-locked to the same phase of the gamma oscillation as pyramidal cells. Current-induced depolarization coupled with synaptically induced inhibition resulted in gamma frequency discharge (30–80 Hz) of pyramidal cells without accommodation. These observations suggest that at least part of the gamma frequency field oscillation reflects rhythmic hyperpolarization of principal cells, brought about by the rhythmically discharging basket neurones. Resonant properties of pyramidal cells might facilitate network synchrony in the gamma frequency range.

Keywords: pyramidal cells, dendrites, basket cells, interneurones, inhibition, resonance, network

Gamma frequency oscillations (> 20 Hz) have been observed in a variety of brain structures of several species (for reviews, see Llinás & Ribary, 1993; Singer, 1993; Gray, 1994; Jefferys *et al*., 1996; Laurent, 1996). These fast oscillations are dominant in the awake, aroused brain and have been implicated in complex functions, e.g. binding of sensory information (Gray *et al*., 1989), consciousness (Llinás & Ribary, 1993), storage of immediate memories (Lisman & Idiart, 1995) and temporal patterning of cortical pyramidal cells (Buzsáki & Chrobak, 1995; Hopfield, 1995). Gamma activity is particularly prominent in the hippocampus and the entorhinal cortex (Stumpf, 1965; Buzsáki *et al*., 1983; Boeijinga & Lopes da Silva, 1989; Skaggs *et al*., 1991; Leung, 1992; Bragin *et al*., 1995; Chrobak & Buzsáki, 1998). The physiological significance of gamma oscillation is that it reflects coordinated activity of neuronal ensembles within a local network and in interconnected distant networks.

The mechanisms underlying gamma oscillations are not fully understood. Studies on the hippocampal formation have suggested that field oscillations in the gamma frequency band reflect synchronous IPSPs on the somata of principal cells (Leung, 1982; Buzsáki *et al*., 1983; Soltész & Deschénes, 1993; Bragin *et al*., 1995; Whittington *et al*., 1995). Intracellular experiments carried out in the thalamus and neocortex, on the other hand, implicate the importance of rhythmic EPSPs as the main source of fast field oscillations (Steriade *et al*., 1996; Steriade & Amzica, 1996; Gray & McCormick, 1996). Population oscillation at gamma frequency may emerge in interneuronal networks even when individual cells fire at different frequencies (Whittington *et al*., 1995; Traub *et al*., 1996a; Wang & Buzsáki, 1996), although intrinsic oscillatory properties of several types of neurones have been demonstrated experimentally (Llinás *et al*., 1991; Gutfreund *et al*., 1995).

In the experiments presented here, we examined the intracellular correlates of field gamma oscillations in anatomically identified pyramidal cells and basket interneurones of the hippocampal CA1 region. Three main questions were addressed. First, whether rhythmic IPSPs play an important role in the generation of field gamma waves and the timing of action potentials in pyramidal cells. Second, whether basket cells maintain spike discharges at gamma frequency and therefore are responsible for the rhythmic somatic IPSPs. Third, whether resonant properties of pyramidal cells may contribute to the network oscillation. The answers to all three questions proved affirmative.

Methods

Forty-six rats of the Sprague–Dawley strain (250–350 g) were anaesthetized with urethane (1.3–1.5 g/kg) and placed in a stereotaxic apparatus. The body temperature of the rat was kept constant by a small animal thermoregulation device. The scalp was removed and a

Correspondence: G. Buzsáki, as above. E-mail: buzsaki@axon.rutgers.edu

Received 14 July 1997, revised 7 October 1997, accepted 16 October 1997

small (1.2 × 0.8 mm) bone window was drilled above the hippocampus (anteromedial edge at AP = –3.3 and L = 2.2 mm from bregma) for extra- and intracellular recordings. The cisterna magna was opened and the cerebrospinal fluid drained to decrease pulsation of the brain. A pair of stimulating electrodes (100 μm each, with 0.5-mm tip separation) was inserted into the left fimbria-fornix (AP = –1.3, L = 1.0, V = 4.1) to stimulate the commissural inputs. Extracellular recording electrodes (two 20-μm insulated tungsten wires) were inserted at the medial edge of the bone window and placed into the CA1 pyramidal layer and the hilus, respectively. Positioning of the recording electrode in the CA1 pyramidal layer was aided by the presence of multiple unit activity and the commissurally evoked responses. After the extracellular and intracellular recording electrodes were inserted into the brain, the bone window was covered by a mixture of paraffin and paraffin oil in order to prevent drying of the brain and decrease pulsation. The distance of the intracellular and extracellular electrodes was 0.5–1.5 mm in the anteroposterior and 0.0–0.5 mm in the lateral directions.

Micropipettes for intracellular recordings were pulled from 2.0-mm capillary glass. They were filled with 1 M potassium acetate in 50 mM Tris buffer (pH = 7.2), also containing 2% biocytin for intracellular labelling. In some experiments, the recording pipette also contained 10 mM of the lidocain derivative QX314 (Sigma, St. Louis, MO). *In vivo* electrode impedances varied from 60 to 100 MΩ. Once stable, intracellular recordings were obtained, evoked and passive physiological properties of the cell determined. Only neurones with a resting potential more negative than –55 mV were included in this study. Since the 'resting' membrane potential fluctuates *in vivo*, we used the amplifier's (Axoclamp-2B; Axon Instruments, Foster City, CA, USA) voltmeter readings to obtain an average value integrated over time. The input resistance of neurones was calculated from steady state membrane responses to hyperpolarizing and depolarizing current steps. A linear regression was fitted to these values.

Field activity recorded through the extracellular electrode was filtered between 1 Hz and 5 kHz. The intracellular activity and the extracellular field/unit activity were digitized at 10 kHz with 12-bit precision (EGAA-16, RC Electronics, Santa Barbara, CA). Intracellular activity was digitized at 10× and 100× amplifications in order to prevent clipping of the action potentials (10×) and at the same time to obtain a high resolution of the membrane potential changes (100×). This procedure was necessary to provide a sufficient digital resolution of the small amplitude membrane voltage oscillations in the gamma frequency band. The electrophysiological data were stored on optical disks.

The data were analysed off-line. The extracellular trace was digitally filtered at 120 dB/octave in order to select the frequency of interest: theta waves (2.5–7 Hz), gamma waves (20–80 Hz) and unit activity (500 Hz–5 kHz) using fast Fourier transformation (FFT). Intracellular spikes were removed digitally. After finding the peak of the action potentials and the membrane potential values 3 ms before and 4 ms after the peak of the spike, the action potential was replaced by a linear fit between these two values. These values were empirically determined and the procedure eliminated the entire action potential and fast spike-afterhyperpolarization. The frequency of gamma activity was determined from the zero-cross intervals of the filtered signal. The filtered intracellular and extracellular traces were full-wave rectified and the peaks of the half-sinus waves or their running averages were displayed as a function of time. For the examination of the relationship between the amplitude of gamma activity and theta cycle, the rectified gamma values were averaged with respect to the positive wave of theta waves. The detected peaks of theta or gamma waves were also used as the zero point for the construction of field averages and cross-correlograms between field activity, extracellular unit activity, intracellular membrane potential changes and action potentials (Ylinen *et al*., 1995). Extracellular units were detected by amplitude discriminator software.

All recordings in this study were made from biocytin-injected and morphologically identified CA1 pyramidal cells. Double and multiple-labelled neurones were discarded from the analysis. After the completion of the physiological data collection, biocytin was injected through a bridge circuit (Axoclamp-2B) using 500 ms depolarizing pulses at 0.6–2 nA at 1 Hz for 10–60 min. Neuronal activity was followed throughout the procedure and the current was reduced if the electrode was blocked and/or the condition of the neurone deteriorated. Two–12 h after the injection, the animals were given an urethane overdose and then perfused intracardially with 100 mL physiological saline followed by 400 mL of 4% paraformaldehyde and 0.2% glutaraldehyde dissolved in phosphate buffered saline (pH = 7.2). The brains were then removed and stored in the fixative solution overnight. Sixty- or 100-μm-thick coronal sections were cut and processed for biocytin labelling. The labelled neurones were reconstructed with the aid of a drawing tube. The histological sections were also used to verify the position of the extracellular recording electrodes and the track made by the recording pipette. Anatomical descriptions of some of the recorded neurones and their physiological behaviour related to theta activity, sharp waves and dentate spikes have been published earlier (Sik *et al*., 1995, 1997; Ylinen *et al*., 1995; Penttonen *et al*., 1997).

For dendritic recordings, the tip of the recording electrode was determined by both physiological and histological methods. Following the withdrawal of the pipette from the dendrite, extracellular-averaged evoked responses to commissural stimulation were obtained at 50-μm steps from the recording site to the pyramidal layer. The polarity reversal of the extracellular field response at the border of strata radiatum and pyramidale provided an additional landmark for the pyramidal layer. The location of dendritic penetration was determined from the distance between the pyramidal layer and the recording site during the experiment, and from the anatomical reconstruction of the electrode track and the dendritic tree of the filled neurone. The pipette was moved up and down several times after its withdrawal from the cell to facilitate histological reconstruction of the electrode track (Kamondi *et al*., 1997).

Results

Gamma frequency oscillation under urethane anaesthesia was most prominent during the presence of hippocampal theta waves (Fig. 1), similar to the EEG activity in the awake animal (Leung *et al*., 1982; Buzsáki *et al*., 1983; Bragin *et al*., 1995). The mean frequency of gamma oscillation was 38 Hz (SD ± 5.8; range 30–48; n = 19 rats). These values are substantially lower than the frequency of gamma in the awake, drug-free animal (Bragin *et al*., 1995). The intracellular analysis presented below was carried out during long epochs of theta/gamma field activity.

Intracellular correlates of gamma frequency oscillation in pyramidal cells

Intracellular recordings from CA1 pyramidal cells revealed membrane potential oscillation in the gamma frequency range (Fig. 1), which was often coherent with the extracellularly recorded field gamma waves. Both the amplitude and phase of intracellular gamma activity were dependent on the polarization level of the neurone. These relationships were investigated in 18 pyramidal neurones that met the

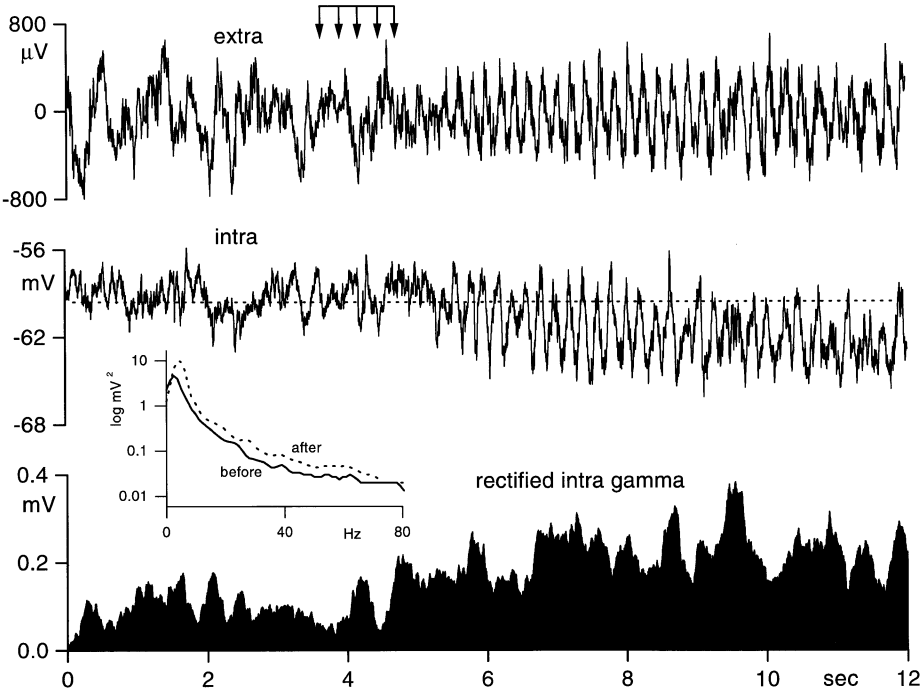

FIG. 1. Amplitude increase of field and intracellular gamma oscillation is associated with theta activity. Simultaneous recording of extracellular field activity in the CA1 pyramidal cell layer and intracellular activity from a pyramidal cell is performed. Theta activity was induced by tail pinching (arrows). The intracellular record was also digitized at 10× larger amplification, filtered for the gamma frequency band (20–80 Hz) and full-wave rectified (rectified intra gamma). Note increased intracellular gamma activity (bottom trace) after the onset of theta waves. Inset: power of intracellular activity before and after the onset of theta activity (logarithmic ordinate). Note increased power in the theta and gamma band during theta state (dashed line, after). The positive polarity of both intracellular and extracellular signals is upward in all figures.

following criteria: overshooting action potentials, resting membrane potential at –60 mV or more negative, frequency of firing less than 2 Hz, stable recording conditions for at least 20 min, presence of regular extracellular theta pattern and histological identification of the neurone after biocytin labelling (Ylinen *et al.*, 1995). The mean input resistance of the included pyramidal cells was 25.4 MΩ (SD ± 10.2; range: 16–42). The mean time constant, as measured at 63% of the maximum response to the –1.0-nA step, was 20.6 ms (SD ± 11.3, range 10–40 ms). Following examination of the passive membrane properties by intracellular current injections, the evoked response properties of the neurone to commissural stimulation were tested. Next, the amplitude and phase-relationship between intracellular and extracellular theta activity was investigated at several intracellular voltage levels.

An example of the voltage dependence of amplitude and phase of intracellular gamma oscillation is illustrated in Figure 2. At resting membrane level, the peak of intracellular depolarization lagged behind the peak positivity of the local extracellular gamma waves by 30–90° in the various cells. The mean intracellular voltage fluctuation in the gamma frequency range varied from 0.2 to 2 mV at resting membrane potential. The amplitude of intracellular gamma increased when the membrane was either hyperpolarized or depolarized. Depolarizations resulted in a larger increase of the intracellular gamma than similar levels of hyperpolarizations in all cases. Upon hyperpolarization, the phase of intracellular gamma remained similar to the extracellular waves. In contrast, when the membrane was depolarized by current injection, the phase shifted or completely reversed (120–180°; Fig. 2B). The voltage dependence of intracellular gamma amplitude and phase was similar to the amplitude minima and polarity reversal of the early IPSPs evoked by the commissural input (Fig. 2C,D). Phase-reversal of both intracellular gamma and the evoked IPSPs occurred between –60 mV and –80 mV. The above changes were consistent in all (n = 18) CA1 pyramidal cells tested.

The voltage dependence of the intracellular gamma amplitude is shown in Figure 3. In this analysis, the filtered gamma activity (20–80 Hz) was rectified and the summed values of the integrated signal were plotted as a function of the intracellular polarization. In order to avoid contamination of action potentials at depolarized levels, they were digitally removed for these calculations. In agreement with the time–domain analysis (Fig. 2), the rectified amplitude of intracellular gamma was lowest at or near the resting membrane potential, and increased when the membrane was either depolarized or hyperpolarized (Fig. 3). In three additional experiments, the recording pipette contained QX-314, a lidocain derivative which is known to block the fast sodium spikes, as well as several potassium channels (Connors & Prince, 1982). The amplitude of filtered gamma waves also continued to increase with depolarization in the presence of QX-314.

Depolarization of the membrane increased the amplitude of gamma activity in the dendrites as well. Dendritic impalements were determined by the smaller amplitude of the action potentials, their decreased rate of rise and decay, increased half-amplitude width, depolarizing spike afterpotentials and resting membrane potentials similar to somatic recordings (< –60 mV, Steriade *et al.*, 1996; Kamondi *et al.*, 1997). In addition, the position of the electrode tip was estimated from the track made by the pipette, the distance from the cell body layer during the experiment and the reconstructed dendritic tree. Changes in gamma activity were examined in three dendritic recordings of CA1 pyramidal cells (Fig. 4). In one of these experiments,

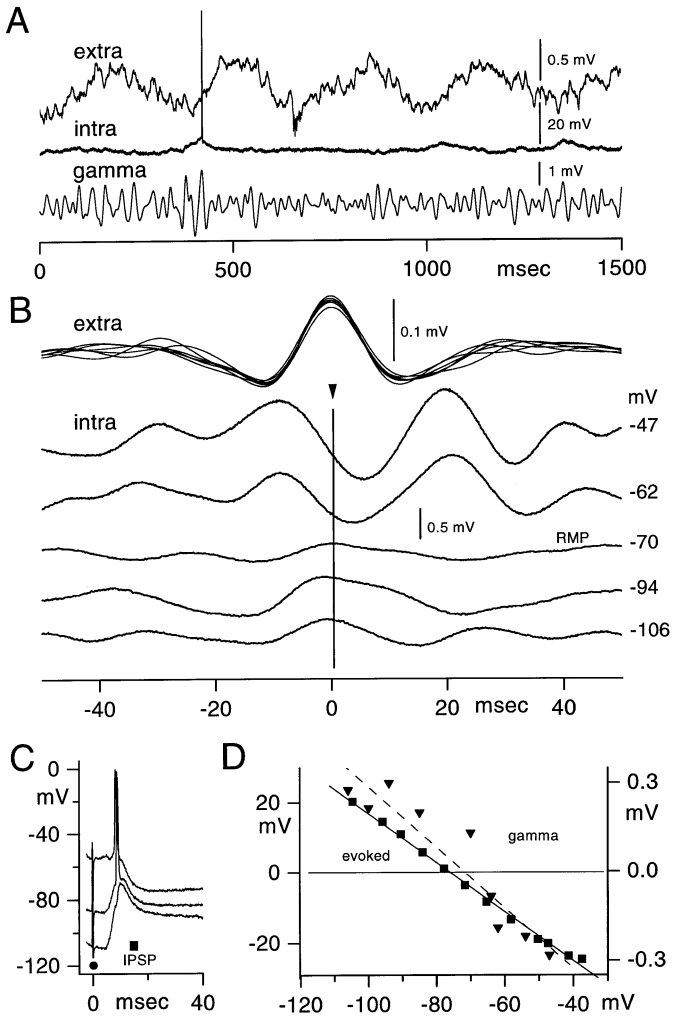

FIG. 2. Voltage dependence of the amplitude and phase of intracellularly recorded gamma activity in a CA1 pyramidal neurone. (A) Simultaneous recording of extracellular theta/gamma activity in the CA1 pyramidal layer (extra) and intracellular voltage fluctuation at resting membrane potential (intra). The intracellular record was also digitized at 10× larger amplification and filtered for the gamma frequency band (20–80 Hz; gamma). (B) Averaged field (superimposed averages; extra) and intracellular traces at various membrane levels. Note increased amplitude of gamma waves at voltage levels above and below resting membrane potential level (RMP, –70 mV) and its phase reversal. (C) Commissural path-evoked responses from the pyramidal cell at three holding potentials. Measurement of the early IPSP is indicated by the square. (D) Amplitude of intracellularly recorded gamma (triangles) and evoked IPSPs (squares) as a function of membrane voltage. Note 'null' zone and phase polarity reversal between –60 and –80 mV in both cases. Averages represent 20–80 repetitions.

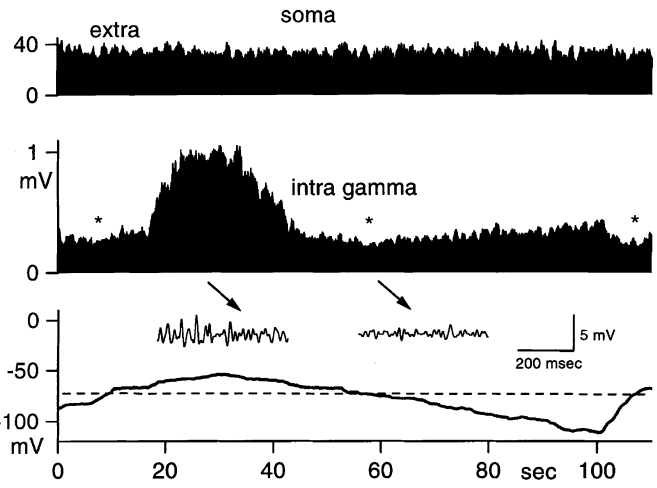

FIG. 3. Voltage dependence of intracellular gamma activity. Continuous display of rectified gamma activity (20–80 Hz) as a function of the membrane potential (intra gamma). The holding current was manually adjusted (bottom trace). The membrane potential induced by the current injection is indicated. Dashed line: zero current. Upper trace: rectified field activity (extra). Note large increase of gamma activity during depolarization and amplitude minima at resting membrane potential (arrows). Insets: filtered segments of intracellular gamma oscillation at times indicated by the arrows. Action potentials were digitally removed.

the recording pipette contained QX 314 (Fig. 4B). Independent of the presence or absence of fast action potentials, the amplitude of intracellular gamma waves increased with membrane depolarization, similar to somatic recordings.

Action potentials of pyramidal neurones tended to be phase-locked to the negative peaks of the extracellularly recorded gamma oscillation. Both cross-correlation of action potential discharges with the extracellular gamma rhythm and spike-triggered averages of the extracellular field indicated that the maximum probability of action potential occurrence lagged 30–90° behind the negative peaks of the gamma waves. This phase relationship, obtained with intracellularly recorded spikes, was identical with the extracellularly recorded multiple unit activity of pyramidal cells (mean = 78° ± 28; see Figs 5 and 8B).

Theta frequency modulation of gamma oscillation

Extracellular recordings in the awake animal have indicated that the fast gamma waves in the dentate gyrus and entorhinal cortex are modulated by the slower frequency theta oscillation (Bragin *et al*., 1995; Chrobak & Buzsáki, 1997). Correlation between the amplitude of gamma waves and the theta cycle also revealed a similar relationship in the CA1 region (Fig. 6). Extracellular gamma activity recorded from the CA1 pyramidal layer showed the largest and smallest amplitude on the positive and negative peaks of the locally derived theta waves, respectively. Intracellular recordings from both somata ($n = 6$) and dendrites ($n = 3$) of pyramidal cells indicated that the membrane oscillation at gamma frequency waxed and waned at similar times with the extracellularly recorded gamma. In the experiment shown in Figure 6(A), somatic and apical dendritic recordings were carried out successively in the same animal. The micropipette contained QX314 in both cases, so the contribution of fast action potentials could be excluded. These experiments indicated that gamma activity in both the somata and dendrites of pyramidal cells was phase-locked to theta activity.

Intracellular correlates of gamma activity in basket neurones

Gamma oscillation-associated intracellular activity has been examined in three anatomically verified CA1 basket cells (UR32 A, UR80B and M63). The histological and some physiological characteristics of these neurones have been published earlier (Sik *et al*., 1995; Ylinen *et al*., 1995). Basket cells responded with multiple spikes to commissural stimulation, and the first action potential preceded the onset of the extracellularly recorded population spike. Reconstruction of the axon arbor of the cells revealed dense innervation of the pyramidal cell bodies. The dendrites were thin and smooth with only occasional spines on the distal dendrites.

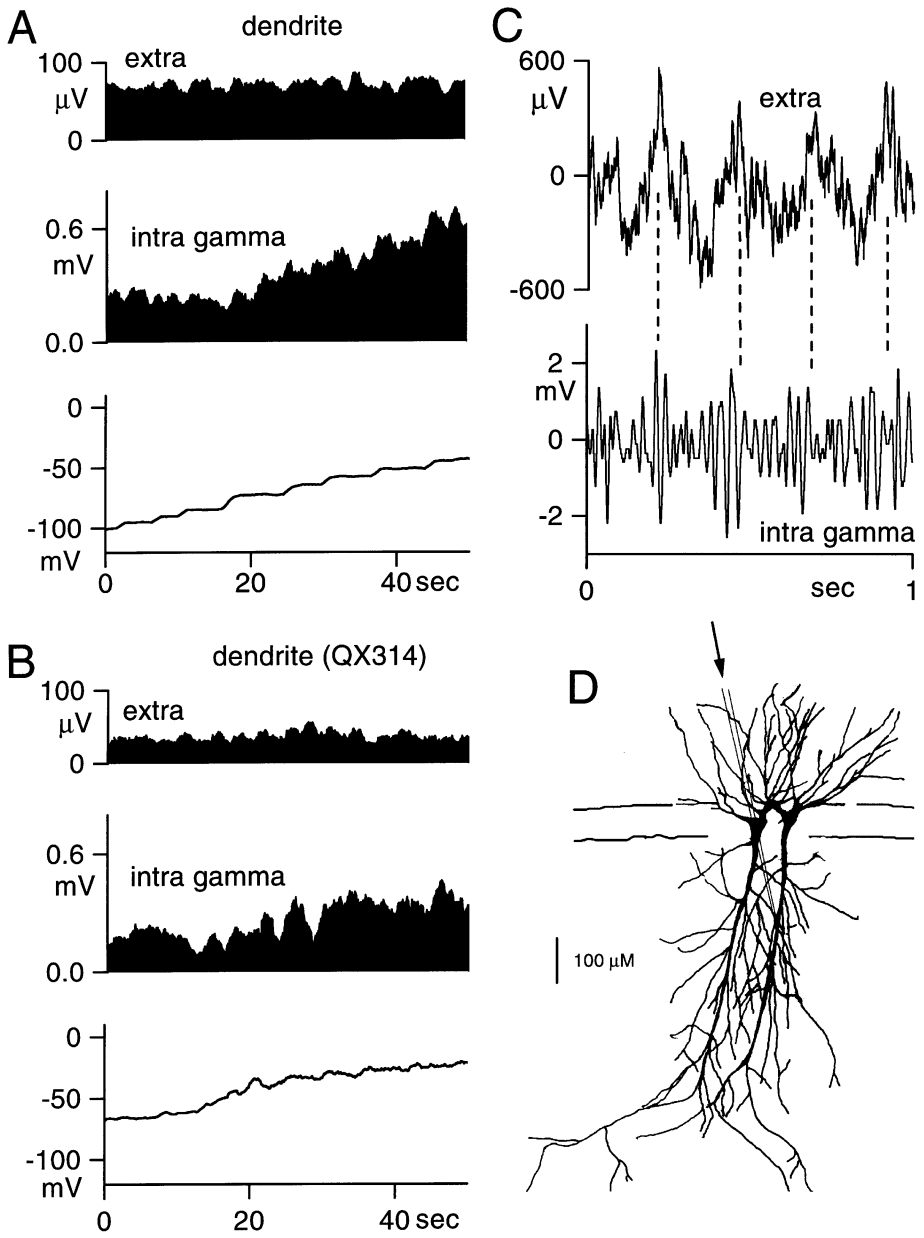

FIG. 4. Gamma activity in apical dendrites of CA1 pyramidal cells. (A) Continuous display of rectified gamma activity (20–80 Hz) as a function of the membrane potential. Action potentials were digitally removed. The holding current was manually adjusted. The dendrite was impaled 320 μm below the pyramidal cell layer (not shown). (B) Similar experiment as in (A), but the pipette also contained QX × 314 (10 mM) to block fast action potentials. (C) Extracellular (extra) and filtered intracellular gamma activity in the dendrite shown in (B) [intra gamma]. (D) Extrapolated position of dendritic impalement for neurone shown in (B) and (C). Drawing tube reconstruction of the biocytin-filled cell and the pipette track. Another neurone was also recorded from the soma in this animal (shown in Fig. 6a).

Basket cells had a characteristic fast spontaneous firing (Figs 7 and 8). At the onset of theta activity the membrane depolarized slightly, which was associated with an increased discharge rate (Fig. 7A). The typical firing pattern of basket cells was characterized by bursts of 20–80 Hz spikes repeated rhythmically at theta frequency (see also Ylinen *et al*., 1995). On average, this pattern corresponded to the theta modulation of extracellular gamma waves. Both cross-correlations and spike-triggered averaging revealed that the action potentials of basket cells were tightly locked to the extracellularly recorded gamma waves (Fig. 8A). The gamma frequency repetition was also evident in their interspike interval histograms. Similar to pyramidal cells, action potentials of basket neurones were phase-locked to the negative portion of the extracellularly recorded gamma oscillation. Both cross-correlation of action potentials with the extracellular gamma rhythm and spike-triggered averages of the extracellular field indicated that the maximum probability of action potential occurrence lagged 30–90° behind the negative peaks of the gamma waves. The maximum probability of firing corresponded to the positive peak of the gamma-associated intracellular depolarization at resting membrane potential (Fig. 7B). Holding potential versus gamma amplitude plots indicated that the amplitude and phase of intracellular gamma was voltage dependent (Fig. 8C).

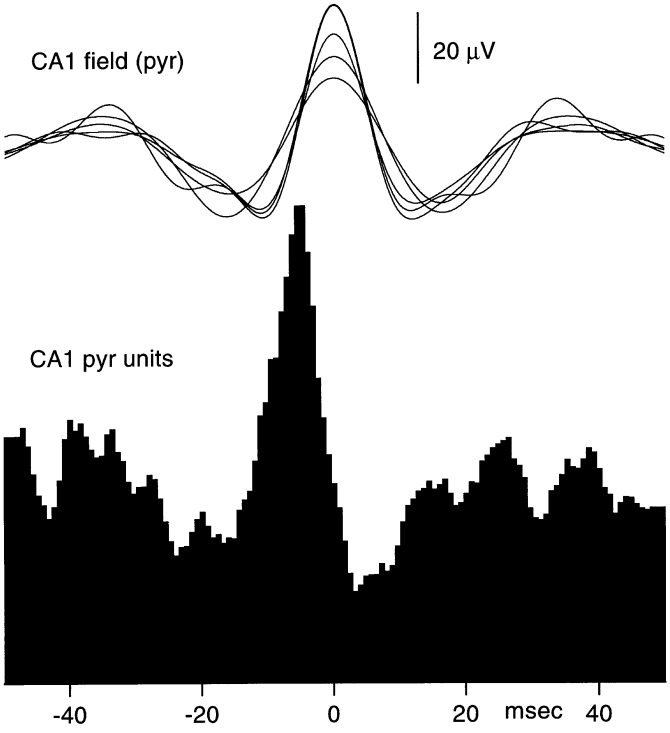

FIG. 5. The occurrence of action potentials in pyramidal cells is timed by gamma oscillation. Averaged gamma waves were recorded from similar positions in the CA1 pyramidal cell layer in five experiments (CA1 field) and their relationship to extracellularly recorded spikes of pyramidal neurones (CA1 pyr units) recorded. The histogram is a grand average of five experiments. Note the peak discharge of the pyramidal cells ⊤ 90° after the local peak negativity of the field gamma.

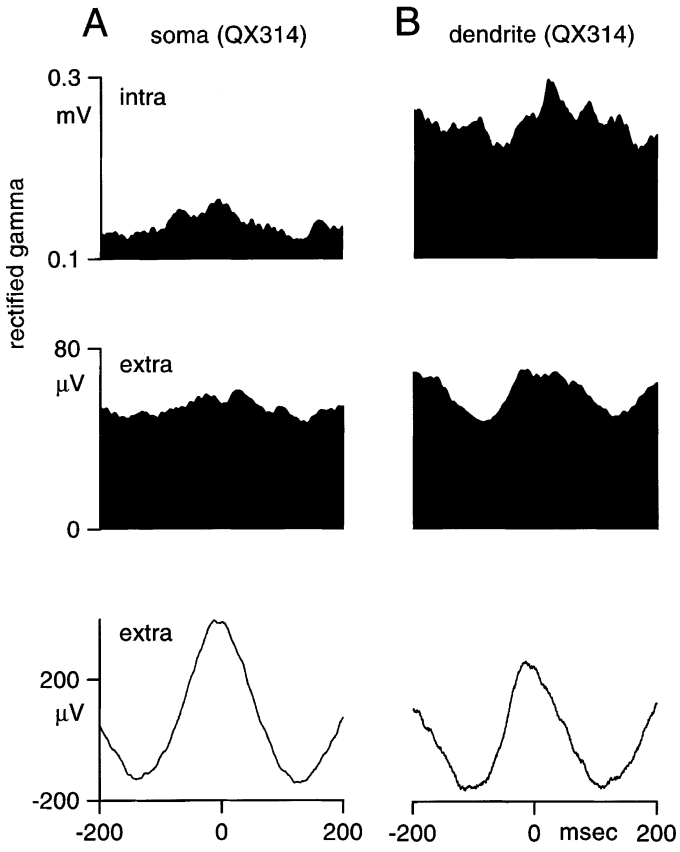

FIG. 6. Theta modulation of gamma activity. Records shown in (A) and (B) were recorded from the soma and dendrite of two pyramidal cells in the same rat (see Fig. 4d). The pipette also contained QX314 to block fast action potentials in both cases. Note increased gamma activity during the positive peak of the locally derived extracellular theta activity in both somatic and apical dendritic recording sites. Bottom trace: averaged theta activity.

Resonant properties of pyramidal cells may contribute to gamma oscillation

The above findings are compatible with the view that gamma oscillations emerge primarily from the network properties of the hippocampal structure. It has remained undisclosed, however, whether intrinsic properties of pyramidal neurone may also contribute to the oscillation. In an attempt to dissociate the intrinsic and network mechanisms, we took advantage of an earlier observation that following single pulse commissural stimulation, firing of both pyramidal cells and interneurones is suppressed for several hundred ms (Buzsáki & Eidelberg, 1982). Such transient post-stimulus periods are likely devoid of fast currents mediated by $GABA_A$, AMPA and NMDA receptors. Thus, we reasoned that the effects of intracellular depolarization can be selectively tested in the absence of network effects during the post-stimulus inhibitory period.

In the absence of commissural stimulation, depolarizing current pulses discharged a train of spikes with increasing interspike intervals in CA1 pyramidal cells. Both the firing frequency and spike frequency accommodation increased as a function of the magnitude of the depolarizing pulse. When repeated responses to identical depolarizing stimuli were superimposed, spike occurrences appeared asynchronously distributed over time. With stronger stimuli, the first few spikes in the train were locked to the onset of depolarization, but the variance of interspike intervals increased afterwards. In contrast, when the same depolarizing steps were preceded by commissural stimulation, they induced rhythmic oscillations of the action potentials (Fig. 9; n = 32 pyramidal cells). Spike frequency accommodation was markedly suppressed and spikes repeated at highly regular intervals. Commissural stimulation was effective in increasing the regularity of spike discharges at any time point after the onset of the depolarizing pulse (Fig. 9A). The frequency and duration of the rhythmic spike trains depended on both the strength of the depolarization pulses, and the amplitude and length of the commissurally evoked inhibition. The spike repetition frequency could be varied between 20 and 80 Hz, with the longest maintained rhythmicity (350 ms) at 30–50 Hz. The frequency of spike oscillation correlated with the magnitude of the depolarizing pulses. Blockade of spike frequency adaptation and the ensuing rhythmic spike discharge were present, irrespective of whether commissural stimulation evoked a monosynaptic spike (Fig. 9F) or not (Fig. 9E). Nevertheless, it was frequently noted that when the stimulus evoked an early, monosynaptically driven spike, it was followed by a more regular spike train than that without the early spike, even though the same stimulus intensity was used. Extracellularly recorded multiple unit activity showed an early increased activity coinciding with the evoked field population spike, but all activity was suppressed for several hundred milliseconds thereafter (Fig. 9D). In eight experiments, we isolated short duration, fast firing putative interneurones (Fox & Ranck, 1981; Buzsáki *et al*., 1983) in the stratum oriens or pyramidale. Only one of these extracellularly recorded putative interneurones discharged a few spikes after the population spike. However, these spikes had no relation to the intracellularly recorded regular action potential train. The averaged evoked field responses also failed to reveal any gamma frequency-

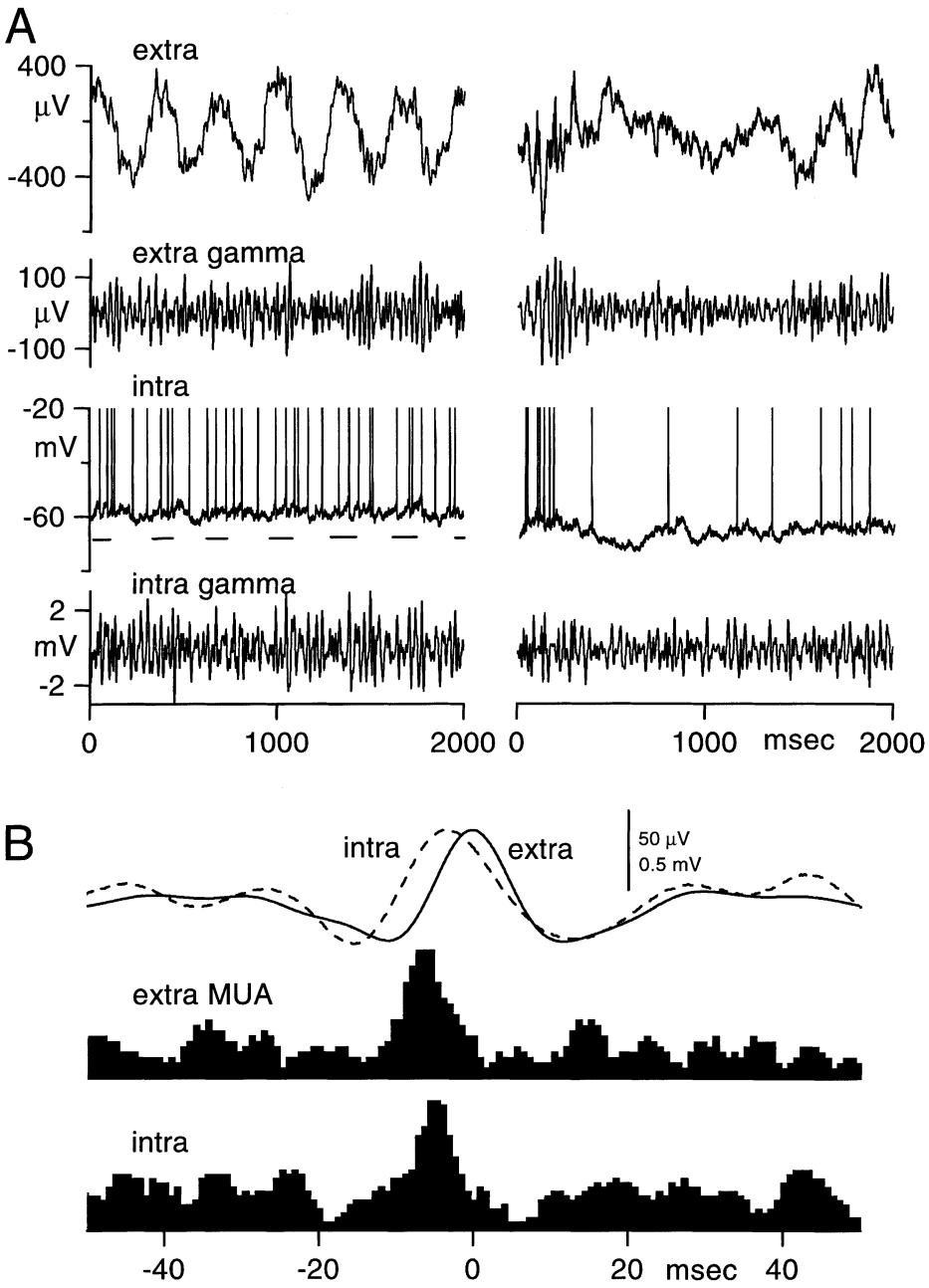

FIG. 7. Network effects on the firing rate and membrane potential of a histologically identified CA1 basket neurone (UR 32 A). (A) Changes in firing rate and filtered membrane oscillation in the basket cell during spontaneous theta to nontheta transition. Approximately 20 s of data was deleted between the left and right traces. Note faster firing rate and larger amplitude oscillation of the membrane potential during extracellular theta/gamma activity. The positive periods of the extracellular theta waves are indicated by horizontal lines under the intracellular trace. Action potentials are clipped. (B) Field gamma-triggered averages of extracellular (extra) and intracellular (intra) voltage traces (20–80 Hz) and cross-correlation between extracellular gamma waves and extracellular multiple unit discharges (extra MUA) and firing of the basket cell (intra). Reference event: positive peak of extracellular gamma waves.

related rhythm at the time when rhythmic discharges occurred in the depolarized pyramidal cell. These observations indicated that it is unlikely that the rhythmic action potentials, recorded intracellularly, were network driven.

Discussion

The main findings of the present experiments are that, in the urethane-anaesthetized rat, (i) the phase and amplitude of intracellular gamma activity are voltage dependent in pyramidal cells and basket cells, (ii) action potentials of pyramidal cells were phase-locked to the population gamma frequency, (iii) resonant properties of pyramidal cells may facilitate gamma-related time locking, (iv) basket cells can discharge at and are phase-locked to gamma frequency, and (v) amplitude of gamma activity is phase-locked to the theta cycle.

Inhibitory potentials contribute to gamma oscillation

In general, field potentials arise from three sources: EPSPs, IPSPs and intrinsic membrane oscillations of individual neurones. The role of EPSPs in the generation of gamma waves has been suggested by

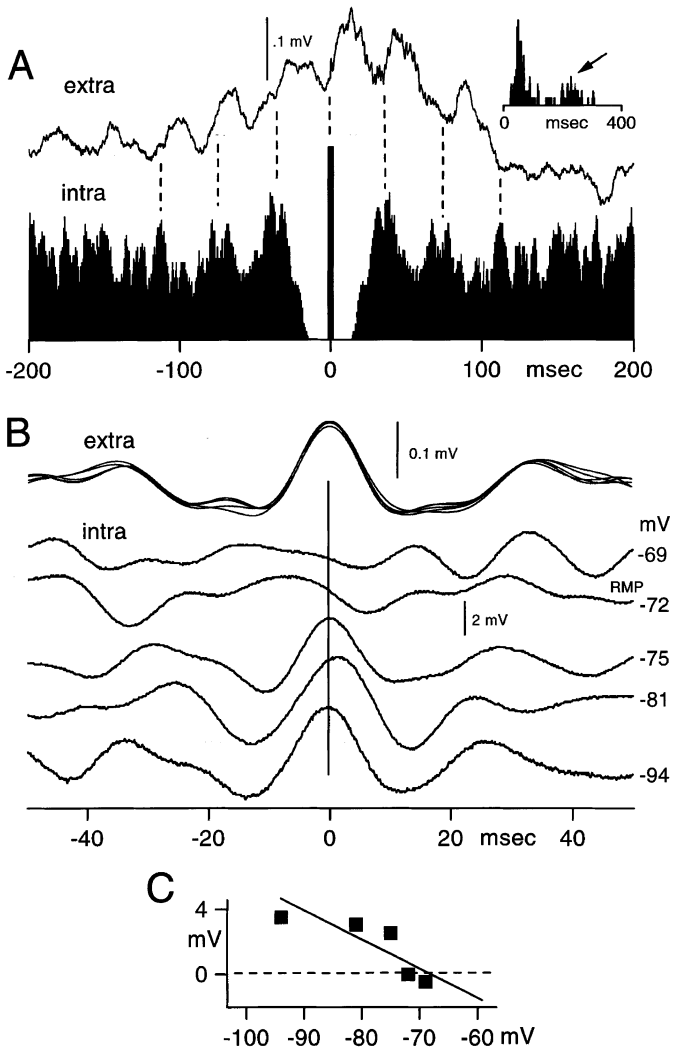

FIG. 8. Basket cells discharge at gamma frequency. (A) Autocorrelogram of spike occurrences (intracellular spikes) and correlated spike-triggered average ($n = 255$) of the wide-band (1 Hz–5 kHz) field activity from the CA1 pyramidal layer. The distance between the intracellular and extracellular electrodes was < 1 mm. Note the rhythmicity of the autocorrelogram and the associated field activity at ⊤ 40 Hz. (B) Field gamma-triggered averages of extracellular (extra; five superimposed average traces) and intracellular (intra) traces (20–80 Hz) from the basket cell (intra; cell UR80B) at different voltage levels. (C) Amplitude of intracellularly recorded gamma as a function of membrane voltage.

several investigators (Stumpf, 1965; Bragin *et al*., 1995; Charpak *et al*., 1995; Steriade *et al*., 1996; Gray & McCormick, 1996). Other works point to the critical role of inhibition (Leung, 1982; Buzsáki *et al*., 1983; Soltész & Deschénes, 1993; Bragin *et al*., 1995). The observations of the present experiments support the hypothesis that at least part of the gamma rhythm recorded in the extracellular space reflects synchronous membrane oscillations in pyramidal cells brought about by rhythmic IPSPs. First, the amplitude of intracellular gamma was smallest between –60 and –80 mV, i.e. in the range of the chloride equilibrium potential. The phase of intracellular oscillation relative to the extracellular gamma rhythm reversed in this voltage range. Second, the voltage-dependent phase and amplitude behaviour of intracellular gamma waves was similar to the amplitude and phase responses of the evoked early (presumably $GABA_A$) IPSPs. Third, histologically identified basket cells innervating the perisomatic region of pyramidal cells discharged at gamma frequency and were phase-locked to the field oscillation. These findings indicate that the charges responsible for the rhythmic gamma waves are mostly carried by chloride ions which enter through $GABA_A$ receptors.

The amplitude of somatically recorded gamma activity varied from 0.2 to 2 mV at resting membrane potential. This range is similar to the unitary IPSPs evoked by a single presynaptic basket or chandelier cell (Buhl *et al*., 1994). Although the input resistance of pyramidal cells is higher *in vitro*, the similar amplitude range of intrasomatic gamma oscillation and IPSPs induced by single interneurones suggests that only a few of the estimated 25 presynaptic basket neurones (Buhl *et al*., 1994) are sufficient to impose a gamma rhythm on pyramidal neurones and time the occurrence of their action potentials. This also implies that concurrently discharging basket and chandelier cells should fire with high temporal precision to avoid interference. Indeed, simultaneously recorded sets of putative basket cells in the awake rat showed zero-time lag in their cross-correlograms (Csicsvari & Buzsaki, unpublished findings). The coordinated burst discharges of the basket cells at gamma frequency as shown here may then induce the larger amplitude theta hyperpolarizations in pyramidal neurones (see also Cobb *et al*., 1995).

Gamma oscillation was also observed in pyramidal cell dendrites. The amplitude of the membrane oscillation was not appreciably smaller than that observed in the soma, suggesting that these fast periodic changes in membrane voltage did not simply passively propagate from the somatic region. Several distinct interneurone types innervate the axon initial segment, somata and dendrites of pyramidal cells (Buhl *et al*., 1994; Sik *et al*., 1995; Freund & Buzsáki, 1996). Although only basket cells were encountered in the present study, other interneuronal types are likely entrained into gamma oscillation (Bragin *et al*., 1995). In the dentate gyrus, several identified interneurone types were phase-locked to the hilar gamma activity (Sik *et al*., 1997), thus it is conceivable that interneurones with dendritic targets in the CA1 region may be responsible for at least part of the observed gamma frequency oscillation in pyramidal cell dendrites.

Resonant properties of pyramidal cells

Hippocampal pyramidal cells are slow firing neurones. Nevertheless, they may transiently increase their firing rates to or above 50 Hz in a variety of behavioural conditions, associated with hippocampal theta/gamma activity (O'Keefe & Recce, 1993; Skaggs *et al*., 1996). After blocking fast synaptic inputs by commissural stimulation, we found that current-induced depolarization of pyramidal neurones resulted in accommodation-free repetitive discharge in the gamma frequency range. The possibility that this rhythmic firing was paced by residual oscillatory activity in the network is unlikely. First, commissural pathway stimulation did not enhance gamma field activity. Second, firing of all pyramidal cells was suppressed for several hundred milliseconds. Third, interneurones were also suppressed (see also Sik *et al*., 1995). Only one of the eight extracellularly recorded interneurones emitted action potentials after the population spike, but these action potentials were not time locked to the intracellular spikes of the depolarized pyramidal cell. Regular firing of pyramidal cells may have been sustained by subthreshold oscillation of the membrane potential, as described in various types of neocortical neurones (Llinás *et al*., 1991; Nunez *et al*., 1992; Gutfreund *et al*., 1995; Gray & McCormick, 1996). The ionic mechanism of gamma frequency oscillation may be different in the various cell types. P/Q types of calcium channels have recently been implicated in subthreshold gamma frequency oscillations of thalamocortical neurones (Pedroarena & Llinas, 1997). An alternative explanation for the regular discharge of pyramidal cells is that the synaptically induced inhibition

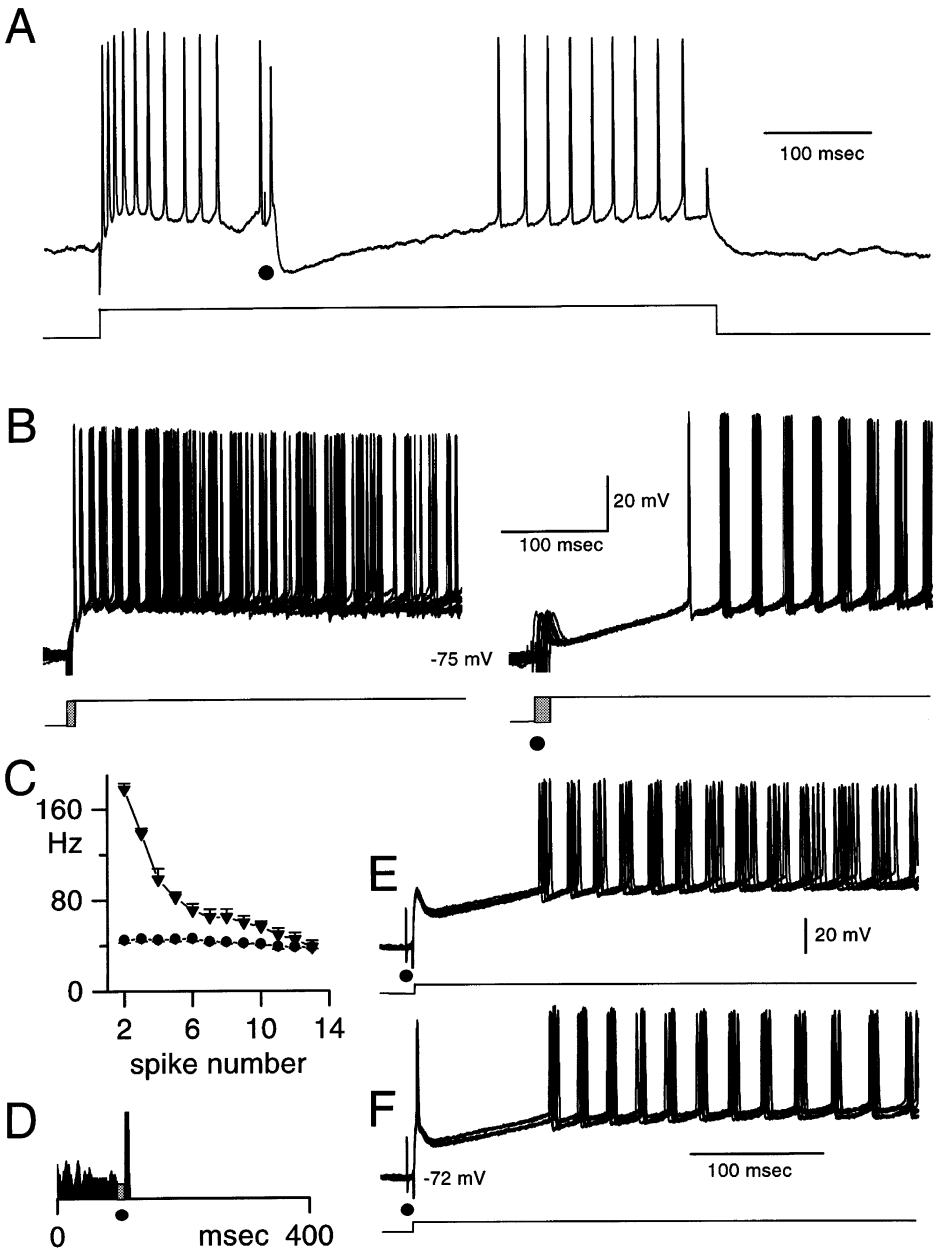

FIG. 9. Resonant properties of pyramidal cells in the gamma frequency range. (A). Response to a current step (0.6 nA) and concurrently applied commissural volley (dot). (B) Superimposed responses of a CA1 pyramidal cell (different from a) to intrasomatic depolarization steps (0.6 nA) without (left) or with (right) a preceding single pulse to the commissural path (dot). The successive responses were aligned relative to the first action potential. Note regular spike discharge at ⊤ 40 Hz after commissural stimulation. (C) Interspike intervals expressed as frequency as a function of spike number in response to depolarizing steps as in (B). Triangles: current steps only; filled circles: currents steps preceded by commissural volleys. Note absence of spike frequency accommodation and regular spike discharge after commissural stimulation. Bars: standard error of mean. (D) Peristimulus time histogram of extracellularly recorded multiple unit activity (n = 20 repetitions). Dot: commissural stimulus. Note complete silence of unit activity after the early evoked response. (E) and (F). Superimposed responses of another CA1 pyramidal cell to intrasomatic depolarization steps (0.6 nA) preceded by commissural path stimulation (dot). Successive responses were grouped depending on whether or not a monosynaptic spike was elicited by the commissural stimulus. Note regular spike discharge at ⊤ 40 Hz, independent of whether the stimulus evoked an initial action potential (F) or not (E), although the regularity of spike discharge was better when stimulation evoked an initial spike.

prevents burst discharge and frequency accommodation of the action potentials. It has recently been shown that activation of interneurones with dendritic targets prevents the occurrence of Ca^{2+} spikes (Buzsáki *et al*., 1996; Miles *et al*., 1996). In the absence of substantial Ca^{2+} influx, Ca^{2+}-mediated K^+ conductance (I_{AHP}, Hotson & Prince, 1980) may not be activated, as reflected by the absence of spike frequency accommodation. In the intact brain, suppression of spike frequency accommodation by inhibition would allow for a high-fidelity transmission of spatial information in pyramidal cells during theta/gamma activity (O'Keefe & Recce, 1993).

Network emergence of the gamma rhythm

Oscillatory behaviour can be maintained, in principle, by mutual excitation, recurrent inhibition or mutual inhibition, or it may be imposed on the network by neurones with pacemaker properties (discussed by Jefferys *et al*., 1996). Various structures may utilize

one or several of these mechanisms. Two important observations put a constraint on these possibilities in the hippocampus. First, pyramidal cells and basket cells discharge on the same phase of the gamma waves, as shown here, in the awake rat and predicted by a model (Bragin *et al*., 1995; Traub *et al*., 1996a). The second is the 'zero-time' lag synchrony of gamma oscillation along the long axis of the hippocampus (Bragin *et al*., 1995). Similar tight synchrony is also observed in the neocortex (Roelfsema *et al*., 1997). A plausible mechanism to account for these experimental data is a separate oscillator (clock) of interconnected interneurones which imposes a rhythmic hyperpolarization on principal cell population and provides a timing reference for phase-coding of neural information (Buzsáki & Chrobak, 1995). Work in the slice preparation and computational experiments support the idea that interneuronal networks in isolation can sustain gamma frequency oscillation via $GABA_A$ receptors (Whittington *et al*., 1995; Traub *et al*., 1996a; Wang & Buzsáki, 1996). The gamma-related IPSPs observed in the basket cells provide support for this hypothesis.

Although basket cells are strongly interconnected, their spatial domain is only ⊤ 1 mm in the CA1 region of the rat hippocampus (Sik *et al*., 1995). It has recently been suggested that large-scale 'zero-time' lag oscillation can be maintained if spatially distant basket cells can be discharged by collaterals of pyramidal cells. Such recurrent/lateral excitation of basket cells is postulated to induce an additional spike during an ongoing gamma cycle (spike 'doublets'), as has been demonstrated in a model of coupled gamma oscillation networks and during stimulation-induced afterdischarges in the slice preparation (Traub *et al*., 1996b). No such spike 'doublets' were evident in our anaesthetized preparation. Nevertheless, pyramidal cells may effectively assist the long-range synchrony of gamma waves by resetting the ongoing gamma frequency discharge of their local and spatially distant interneurone targets. Alternatively, large scale interneurone networks with axon collaterals reaching distant structures may provide a clock for synchronizing the discharges of spatially distant principal cells (Buzsáki & Chrobak, 1995). Gamma oscillations observed in the dendrites of pyramidal cells and the existence of inhibitory interneurones with long-range axonal projections (Sik *et al*., 1994, 1995) provide support for this hypothesis.

Acknowledgements

László Acsády, Anita Kamondi and Markku Penttonen were visiting scholars at Rutgers University. We thank Dr Aarne Ylinen and Dr Attila Sik for performing some of the experiments. This work was supported by NINDS (NS34994), NIMH (MH54671), the Human Frontier Science Program, Finnish Academy of Sciences (32391) (M. P.), the Soros Foundation (L. A. and A. K.) and the Whitehall Foundation.

Abbreviations

AMPA	α-amino-3-hydroxy-5-methyl-4-isoxazole propionic acid
EPSP	excitatory postsynaptic potential
GABA	γ-aminobutyric acid
IPSP	inhibitory postsynaptic potential
NMDA	*N*-methyl-D-aspartic acid
QX-314	N-(2,6-dimethylphenylcarbamoylmethyl)triethylammonium bromide

References

Boeijinga, P.H. & Lopes da Silva, F.H. (1989) Modulations of EEG activity in the entorhinal cortex and forebrain olfactory areas during odour sampling. *Brain Res.*, **478**, 257–268.

Bragin, A., Jando, G., Nadasdy, Z., Hetke, J., Wise, K. & Buzsáki, G. (1995) Gamma frequency (40–100 Hz) patterns in the hippocampus of the behaving rat. *J. Neurosci.*, **15**, 47–60.

Buhl, E.H., Halasy, K. & Somogyi, P. (1994) Diverse sources of hippocampal unitary inhibitory postsynaptic potentials and the number of synaptic release sites. *Nature*, **368**, 823–828.

Buzsáki, G. & Chrobak, J.J. (1995) Temporal structure in spatially organized neuronal ensembles: a role for interneuronal networks. *Curr. Opin. Neurobiol.*, **5**, 504–510.

Buzsáki, G. & Eidelberg, E. (1982) Direct afferent excitation and long-term potentiation of hippocampal interneurons. *J. Neurophysiol.*, **48**, 597–607.

Buzsáki, G., Leung, L. & Vanderwolf, C.H. (1983) Cellular bases of hippocampal EEG in the behaving rat. *Brain Res. Rev.*, **6**, 139–171.

Buzsáki, G., Penttonen, M., Nádasdy, Z. & Bragin, A. (1996) Pattern and inhibition-dependent invasion of pyramidal cell dendrites by fast spikes in the hippocampus *in vivo*. *Proc. Natl. Acad. Sci. USA*, **93**, 9921–9925.

Charpak, S., Paré, D. & Llinás, R. (1995) The entorhinal cortex entrains fast CA1 hippocampal oscillations in the anaesthetized guinea-pig: role of the monosynaptic component of the perforant path. *Eur. J. Neurosci.*, **7**, 1548–1557.

Chrobak, J.J. & Buzsáki, G. (1998) Gamma oscillation in the entorhinal-hippocampal axis of the freely behaving rat. *J. Neurosci.*, in press.

Cobb, S.R., Buhl, E.H., Halasy, K., Paulsen, O. & Somogyi, P. (1995) Synchronization of neuronal activity in hippocampus by individual GABAergic interneurons. *Nature*, **378**, 75–98.

Connors, B.W. & Prince, D.A. (1982) Effects of the local anesthetic QX-314 on the membrane properties of hippocampal pyramidal neurons. *J. Pharmacol. Exp. Ther.*, **220**, 476–481.

Fox, S.E. & Ranck, J.B. Jr (1981) Electrophysiological characteristics of hippocampal complex-spike cells and theta cells. *Exp. Brain Res.*, **41**, 299–313.

Freund, T.F. & Buzsáki, G. (1996) Interneurons of the hippocampus. *Hippocampus*, **6**, 347–470.

Gray, C.M. (1994) Synchronous oscillations in neuronal systems: mechanisms and functions. *Comput. Neurosci.*, **1**, 11–38.

Gray, C.M., Koenig, P., Engel, A.K. & Singer, W. (1989) Stimulus-specific neuronal oscillations in cat visual cortex exhibit inter-columnar synchronization which reflects global stimulus properties. *Nature*, **338**, 334–337.

Gray, C.M. & McCormick, D.A. (1996) Chattering cells: superficial pyramidal neurons contributing to the generation of synchronous oscillations in the visual cortex. *Science*, **274**, 109–113.

Gutfreund, Y., Yarom, Y. & Segev, I. (1995) Subthreshold oscillations and resonant frequency in guinea-pig cortical neurons: physiology and modelling. *J. Physiol. (Lond.)*, **483**, 621–640.

Hopfield, J.J. (1995) Pattern recognition computation using action potential timing for stimulus representation. *Nature*, **376**, 33–36.

Hotson, J.R. & Prince, D.A. (1980) A calcium-activated hyperpolarization follows repetitive firing in hippocampal neurons. *J. Neurophysiol.*, **43**, 409–419.

Jefferys, J.G.R., Traub, R.D. & Whittington, M.A. (1996) Neuronal networks for induced '40 Hz' rhythms. *Trends. Neurosci.*, **19**, 202–208.

Kamondi, A., Acsády, L. & Buzsáki, G. (1997) Dendritic spikes are enhanced by cooperative network activity in the intact hippocampus. *Soc. Neurosci. Abstr.*, 263.10.

Laurent, G. (1996) Dynamical representation of odors by oscillating and evolving neural assemblies. *Trends. Neurosci.*, **19**, 489–496.

Leung, L.S. (1982) Nonlinear feedback model of neuronal populations in hippocampal CAl region. *J. Neurophysiol.*, **47**, 845–868.

Leung, L.S. (1992) Fast (beta) rhythms in the hippocampus: a review. *Hippocampus*, **2**, 93–98.

Leung, L.S., Lopes da Silva, F.H. & Wadman, W.J. (1982) Spectral characteristics of the hippocampal EEG in the freely moving rat. *Electroencephal. Clin. Neurophysiol.*, **54**, 203–219.

Lisman, J.E. & Idiart, M.A.P. (1995) A mechanism for storing 7±2 short-term memories in oscillatory subcycles. *Science*, **267**, 1512–1514.

Llinás, R.R., Grace, A.A. & Yarom, Y. (1991) In vitro neurons in mammalian cortical layer 4 exhibit intrinsic oscillatory activity in the 10- to 50-Hz frequency range. *Proc. Natl. Acad. Sci. USA*, **88**, 897–901.

Llinás, R. & Ribary, U. (1993) Coherent 40-Hz oscillation characterizes dream state in humans. *Proc. Natl. Acad. Sci. USA*, **90**, 2078–2081.

Miles, R., Tóth, K., Gulyás, A.I., Hájos, N. & Freund, T.F. (1996) Differences between somatic and dendritic inhibition in the hippocamus. *Neuron.*, **16**, 815–823.

Nunez, A., Amzica, F. & Steriade, M. (1992) Voltage-dependent fast (20–40 Hz) oscillations in long-axoned neocortical neurons. *Neuroscience*, **51**, 7–10.

O'Keefe, J. & Recce, M.L. (1993) Phase relationship between hippocampal place units and the EEG theta rhythm. *Hippocampus*, **3**, 317–330.
Pedroarena, C. & Llinas, R. (1997) Dendritic calcium conductances generate high-frequency oscillation in thalamocortical neurons. *Proc. Natl. Acad. Sci. USA*, **94**, 724–728.
Penttonen, M., Kamondi, A., Sik, A., Acsády, L. & Buzsáki, G. (1997) Feed-forward and feed-back activation of the dentate gyrus *in vivo*: dentate EEG spikes and sharp wave bursts. *Hippocampus*, **7**, 437–450.
Roelfsema, P.R., Engel, A.K., König, P. & Singer, W. (1997) Visuomotor integration is associated with zero time-lag synchronization among cortical areas. *Nature*, **385**, 157–161.
Sik, A., Penttonen, M. & Buzsáki, G. (1997) Interneurons in the hippocampal dentate gyrus: an *in vivo* intracellular study. *Eur. J. Neurosci.*, **9**, 573–588.
Sik, A., Penttonen, M., Ylinen, A. & Buzsáki, G. (1995) Hippocampal CA1 interneurons: an *in vivo* intracellular labeling study. *J. Neurosci.*, **15**, 6651–6665.
Sik, A., Ylinen, A., Penttonen, M. & Buzsáki, G. (1994) Inhibitory CA1-CA3-hilar region feedback in the hippocampus. *Science*, **265**, 1722–1724.
Singer, W. (1993) Synchronization of cortical activity and its putative role in information processing and learning. *Ann. Rev. Physiol.*, **55**, 349–374.
Skaggs, W.E., McNaughton, B.L. & Barnes, C.L. (1991) 40-Hz 'fluttering' oscillation in the rat hippocampus. *Soc. Neurosci. Abstr.*, **17**, 1395.
Skaggs, W.E., McNaughton, B.L., Wilson, M.A. & Barnes, C.A. (1996) Theta phase precession in hippocampal neuronal populations and the compression of temporal sequences. *Hippocampus*, **6**, 149–173.
Soltész, I. & Deschénes, M. (1993) Low- and high-frequency membrane potential oscillations during theta activity in CA1 and CA3 pyramidal neurons of the rat hippocampus under ketamine-xylazine anesthesia. *J. Neurophysiol.*, **70**, 97–116.
Steriade, M. & Amzica, F. (1996) Intracortical and corticothalamic coherency of fast spontaneous oscillations. *Proc. Natl. Acad. Sci. USA*, **93**, 2533–2538.
Steriade, M., Amzica, F. & Contreras, D. (1996) Synchronization of fast (30–40 Hz) spontaneous cortical rhythms during brain activation. *J. Neurosci.*, **16**, 392–417.
Stumpf, C. (1965) Drug action on the electrical activity of the hippocampus. *Int. Rev. Neurobiol.*, **8**, 77–138.
Traub, R.D., Whittington, M.A., Colling, S.B., Buzsáki, G. & Jefferys, J.G. (1996a) Analysis of gamma rhythms in the rat hippocampus *in vitro* and *in vivo. J. Physiol. (Lond.)*, **493**, 471–484.
Traub, R.D., Whittington, M.A., Stanford, I.M. & Jefferys, J.G. (1996b) A mechanism for generation of long-range synchronous fast oscillations in the cortex. *Nature*, **383**, 621–624.
Wang, X.-J. & Buzsáki, G. (1996) Gamma oscillation by synaptic inhibition in an interneuronal network model. *J. Neurosci.*, **16**, 6402–6413.
Whittington, M.A., Traub, R.D. & Jeffreys, J.G.R. (1995) Synchronized oscillation in interneuron networks driven by metabotropic glutamate receptor activation. *Nature*, **373**, 612–615.
Ylinen, A., Soltész, I., Bragin, A., Penttonen, M., Sik, A. & Buzsáki, G. (1995) Intracellular correlates of hippocampal theta rhythm in identified pyramidal cells, granule cells and basket cells. *Hippocampus*, **5**, 78–90.